NEW ZEALAND SOCIETY FOR EARTHQUAKE ENGINEERING
2019 Pacific Conference on Earthquake Engineering
TURNING HAZARD AWARENESS INTO RISK MITIGATION
4 – 6 April | SkyCity, Auckland | New Zealand

Non-linear behaviour of welded stitch plate connections in jointed precast building cores

S.J. Menegon
Swinburne University of Technology and Wallbridge Gilbert Aztec, Melbourne, Australia.

J.L. Wilson
Swinburne University of Technology, Melbourne, Australia.

N.T.K. Lam
University of Melbourne, Melbourne, Australia.

E.F. Gad
Swinburne University of Technology, Melbourne, Australia.

ABSTRACT

Reinforced concrete (RC) walls and building cores are widely used lateral load resisting systems for low, mid and high-rise buildings in lower seismic regions, such as Australia. Traditionally, RC walls and cores were constructed using monolithic cast in-situ elements. However, in recent years, precast concrete walls and cores have become increasingly popular, particularly jointed precast building cores. Precast building cores consist of individual rectangular panels that are cast off-site and then transported and erected on-site. The panels are connected together using welded stitch plate (WSP) connections, which are used to transfer vertical shear forces between adjacent panels to allow the individual panels to act compositely together as one element. This paper presents the findings of a recent experimental and analytical study into the performance and behaviour of WSP connections in jointed precast building cores in lower seismic regions. The paper will initially provide an overview of the experimental assessment performed on a typical WSP connection using the MAST system at Swinburne University of Technology. The paper will then conclude with an introduction into the current analytical work currently being performed to better understand the behaviour of these connections.

Paper 307

1 INTRODUCTION

The authors have been undertaking a long-term Australian Research Council (ARC) funded research program to assess and reduce the seismic risk and rationalise the seismic design procedures and practices in Australia. While the primary focus is Australia, the research outcomes and findings are relevant to most regions of lower seismicity around the world. The current/ongoing research objective is to assess and quantify the seismic performance of limited ductile RC wall buildings, which are locally in Australia, the dominant form of construction for low, mid and high-rise multi-storey buildings (Menegon et al. 2017c). One of the primary objectives of the project is to better understand the non-linear post-peak behaviour and collapse displacement of limited ductile RC wall systems, since the sole design objective for earthquake actions in Australia is collapse prevention, for the majority of structures (Menegon et al. 2018b).

The design and detailing of limited ductile buildings in the Australia is somewhat comparable to non-ductile construction in higher seismic regions such as New Zealand or the west coast of the United States. RC wall buildings in Australia traditionally utilised monolithic cast in-situ rectangular walls and/or buildings cores. Where the latter typically consisted of box shaped elements around lift shafts or emergency exit stairwells. However, in recent years, the adoption of precast walls and building cores has rapidly increased. Precast wall systems are also widely used in New Zealand (Seifi, Henry and Ingham 2016). Precast wall systems typical of Australia construction practices have received little research attention, relative to cast in-situ walls, and as such, their behaviour and performance has largely been assessed theoretically in structural design offices.

The authors, as part of the ongoing research project discussed above, have completed an experimental testing program comprising three large-scale jointed precast building core specimens (Menegon 2018; Menegon et al. 2017b). Additionally, the authors have also undertaken experimental assessments of three different types of precast building core panel-to-panel connections (Menegon 2018; Menegon et al. 2017a; Menegon et al. 2018a). The later included a typical welded stitch plate (WSP) connection and the development of two new innovative prototype connections (i.e. the ‘grouted panel pocket’ (GPP) connection and the ‘post tensioned corbel’ (PTC) connection). This paper will provide a brief overview of the WSP connection specimen, the experimental results and the ongoing analytical assessments being undertaken.

2 EXPERIMENTAL TESTING

2.1 Test methodology and specimen details

The WSP connection specimen (denoted J01), as shown in Figure 3, was an exact replication of the WSP connections used to construct one of the largescale system level building core specimens (i.e. S05) tested by the authors and further presented in Menegon (2018) or Menegon et al. (2017b). Specimen S05 was meant to represent the first storey segment of a taller four-storey building core. This specimen was tested under combined in-plane cyclic lateral displacements, constant axial load (which was approximately equal to an axial load ratio of 5%) and an in-plane bending moment coupled to the lateral force capacity. This allowed the one-storey test specimen to have the equivalent response as the first storey of a taller four-storey specimen, as illustrated in Figure 1.

Specimen J01 was effectively then the corner segment of S05, as illustrated in Figure 2, which consisted of two WSP connections (one top and one bottom). It was tested using the Multi-Axis Substructure Testing (MAST) System at Swinburne University of Technology. The specimen was subject to cyclic vertical displacements with the base of one panel fixed to the strong floor in the laboratory and the top of the adjacent panel fixed to the crosshead of the MAST System. The top of the former and the bottom of the later were restrained using structural steel brackets with slotted holes that resisted/prevented the development of eccentric forces from the test setup (refer Menegon (2018) for further details). This allowed the connection to be subjected to pure vertical shear forces, representative of what would occur in system level response.

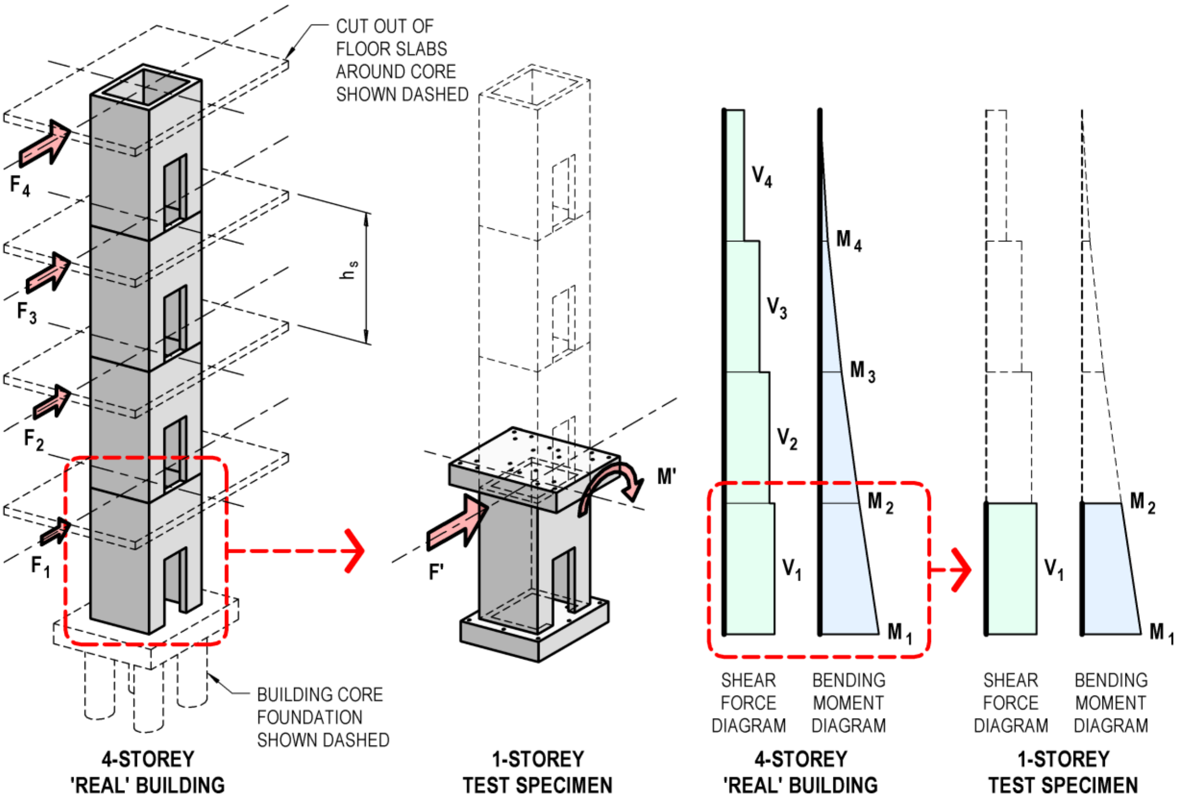

Figure 1: System level testing (Menegon et al. 2017b).

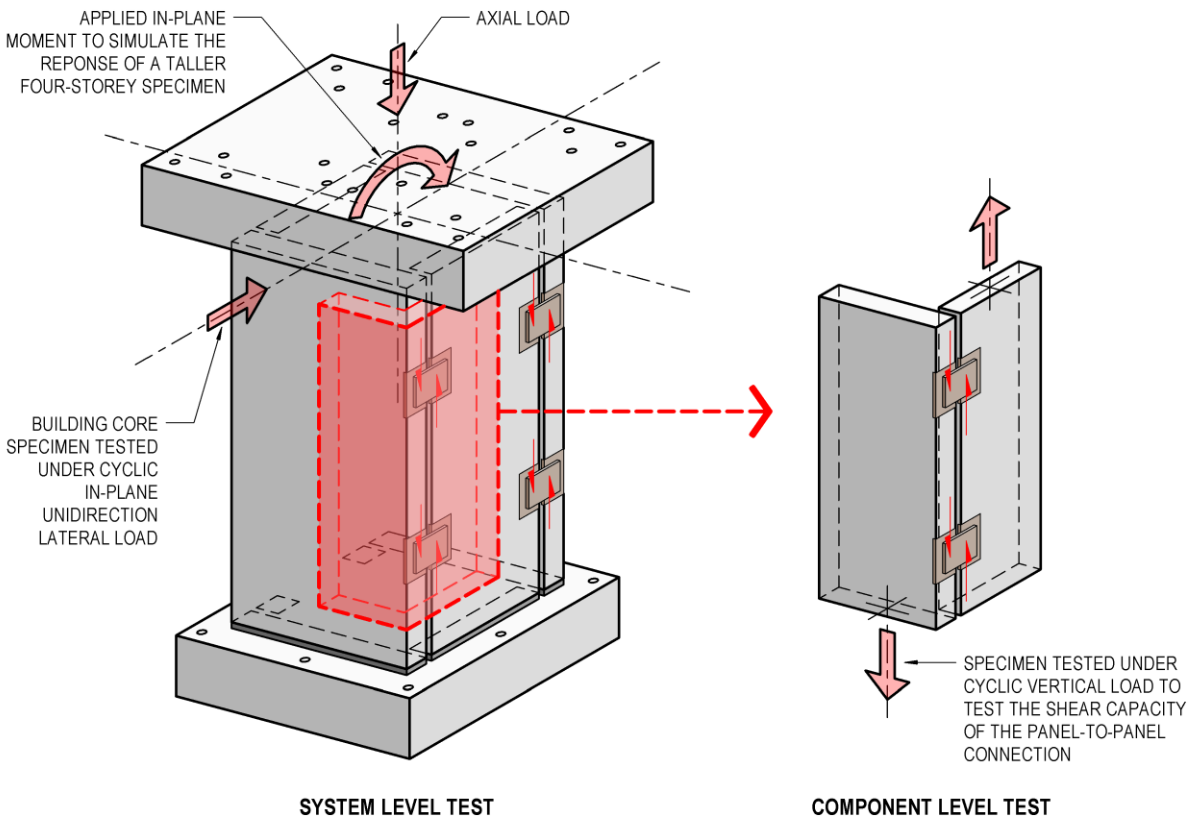

Figure 2: Component level testing (Menegon et al. 2017a).

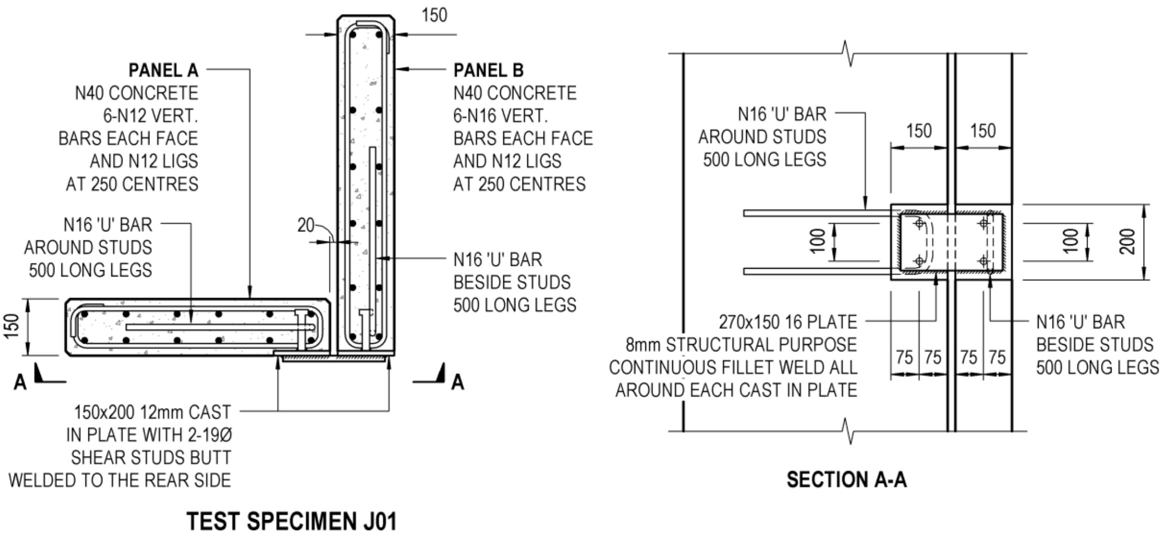

Figure 3: Welded stitch plate connection specimen (i.e. J01).

2.2 Test results

Specimen J01 had a maximum strength of 176 and 177 kN in the positive and negative loading directions respectively. The overall force-displacement behaviour of the connection is presented in Figure 4 (left) and the local behaviour of a single connection is presented in Figure 4 (right). The latter only shows the first two loading cycle series for clarity. The top and bottom connection had approximately the same vertical displacement across the duration of the test, and as such, the force was assumed to be evenly distributed between the top and bottom connection.

The stiffness of the connection was taken as a secant stiffness from the origin to point a corresponding to 70% of the maximum capacity of the connection being reached. A value of 70% was selected because this represents approximately 80% of the design capacity (e.g. the capacity reduction factor for a shear stud in accordance with AS 2327.1 (Standards Australia 2003) is 0.85 and 0.8 x 0.85 ~ 0.7) and Menegon (2018) recommends precast core connections be limited to 80% of their capacity in design.

The connection therefore had a positive and negative stiffness of 36.4 and 52.5 kN/mm respectively. The overall connection stiffness was taken as the average of these two values, i.e. 44.5 kN/mm.

The WSP connections exhibited a reasonably ductile failure mode, allowing a fair amount of connection deformation and gradual decline in strength. The failure mechanism was yielding and fracturing of the shear studs. As such, the maximum vertical shear strength of the connection was directly proportionate to the ultimate shear strength of the studs.

The vertical force is transferred between the adjacent panels through the centroid of the respective shear stud groups. This creates a couple that is equal to the vertical force multiplied by half the distance between the centroid of the shear stud group on each respective panel (refer Figure 5). The couple is resisted on each side of the connection by opposing horizontal forces on the top and bottom shear stud. The magnitude of the horizontal force that acts on each stud is dependent on the geometry of the connection. The shear studs have a vertical force applied to them that is equal to half of the vertical force transferred across the connection. The resultant shear force applied to the shear studs can therefore be calculated using Equation 1.

The maximum load of each WSP connection was approximately 88 kN. Therefore, using Equation 1, the maximum resultant shear force acting on the shear studs was 87 kN. The maximum capacity of 19 mm diameter shear stud, determined in accordance with AS 2327.1, is 93 kN. This is somewhat in good agreement with the results of J01.

$$F = F_{y,1} + F_{y,2}$$

$$M = F \times \left(\frac{170}{2}\right)$$

$$F_{y,1} = 0.5F$$

$$F_{x,1} = \frac{M}{100} = \frac{85F}{100} = 0.85F$$

$$F_{R,1} = \sqrt{\left(F_{x,1}\right)^2 + \left(F_{y,1}\right)^2} = \sqrt{(0.85F)^2 + (0.5F)^2} = 0.99F$$

$$\therefore \ [F]_{max} = 1.01 \times \left[F_{R,1}\right]_{max} \tag{1}$$

Where: $[F]_{\max}$ is the maximum vertical shear strength of the connection; and $\left[F_{R,1}\right]_{\max}$ is the maximum shear capacity of the shear studs.

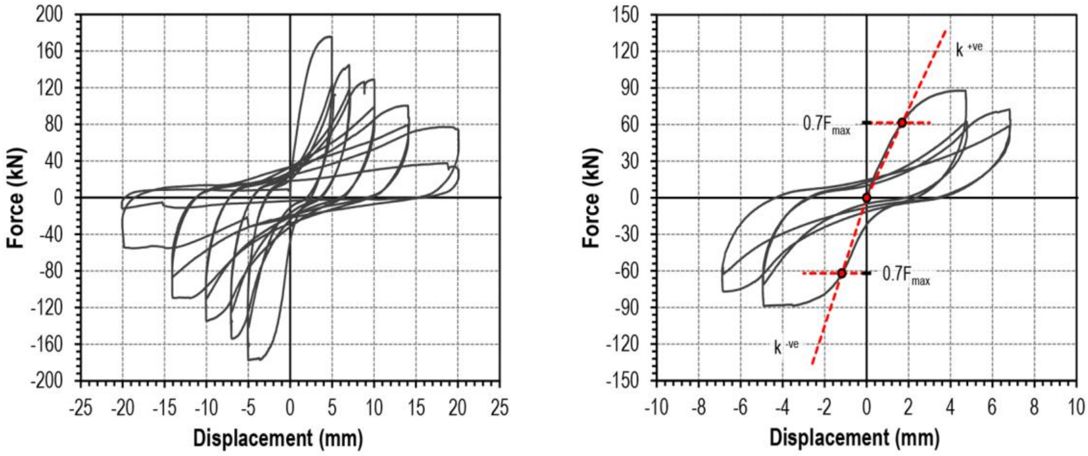

Figure 4: Force-displacement behaviour of the overall specimen (left) and single WSP connection (right).

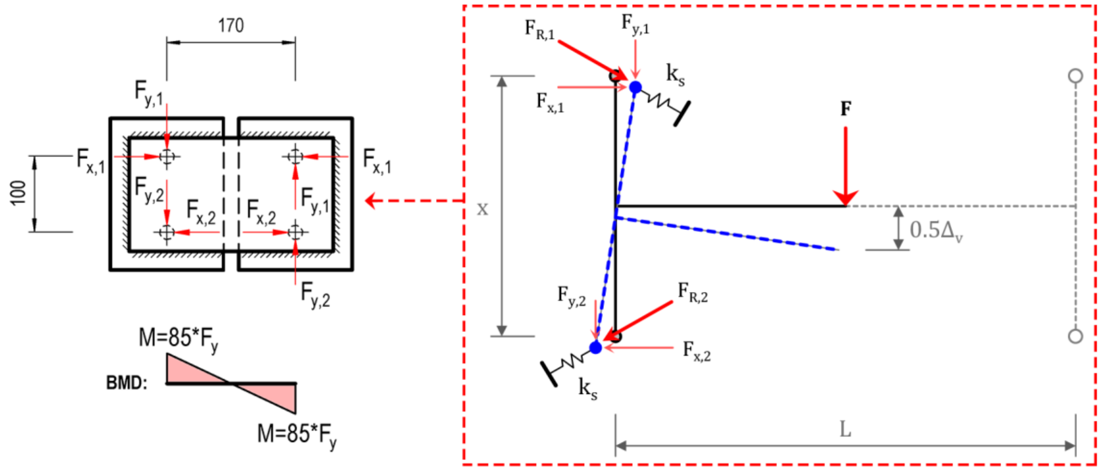

Figure 5: Shear stud forces (left) and deflected shape with resultant forces and stud springs (right).

3 NON-LINEAR RESPONSE AND STIFFNESS OF THE SHEAR STUDS

It was observed during the large-scale system level testing of building core specimen S05 that the connections were not stiffness enough to develop full composite action in the section Menegon (2018); the specimen only developed 80% of the theoretical maximum moment capacity corresponding to full composite behaviour and it was also 25% more flexible than the equivalent cast in-situ section. The following models were developed to better understand and assess the stiffness of WSP connections.

The displacement behaviour of the WSP connection in J01 was predominantly due to rigid body rotation of the overall connection, with negligible shear or flexural displacement from the stitch plate itself (Menegon 2018). The rigid body rotation was due to the movement between the shear studs and the concrete. As such, the displacement of the connection can be expressed using the x- and y-axis displacement components of each shear stud, i.e. Equation 2.

$$0.5\Delta_v = 0.5(\Delta_{y,1} + \Delta_{y,2}) + (\Delta_{x,1} - \Delta_{x,2})(0.5L/x) \quad (2)$$

Where: Δ_v is the vertical displacement of the connection; $\Delta_{y,1}$ and $\Delta_{y,2}$ are the y-axis displacements at shear studs 1 and 2 respectively; $\Delta_{x,1}$ and $\Delta_{x,2}$ are the x-axis displacements at shear studs 1 and 2 respectively; L is the distance between the centroid of the shear stud group on each respective panel; and x is the vertical distance between the shear studs.

The x- and y-axis displacement components can be expressed in terms of the forces acting on each shear and the stiffness of the shear studs (i.e. k_s). The forces on each shear are determined using simple mechanics. As such, Equations 3–9 below can be derived.

$$\Delta_{R,1} = F_{R,1}/k_s \quad \text{and} \quad \Delta_{R,2} = F_{R,2}/k_s \quad (3)$$

$$F_{R,1} = \sqrt{{F_{x,1}}^2 + {F_{y,1}}^2} \quad \text{and} \quad F_{R,2} = \sqrt{{F_{x,2}}^2 + {F_{y,2}}^2} \quad (4)$$

$$F_{x,1} = F(0.5L/x) \quad \text{and} \quad F_{x,2} = -F(0.5L/x) \quad (5)$$

$$F_{y,1} = 0.5F \quad \text{and} \quad F_{y,2} = 0.5F \quad (6)$$

$$\theta_{R,1} = tan^{-1}(F_{y,1}/F_{x,1}) \quad \text{and} \quad \theta_{R,2} = tan^{-1}(F_{y,2}/F_{x,2}) \quad (7)$$

$$\Delta_{x,1} = \Delta_{R,1}\, cos\, \theta_{R,1} \quad \text{and} \quad \Delta_{x,2} = \Delta_{R,2}\, cos\, \theta_{R,2} \quad (8)$$

$$\Delta_{y,1} = \Delta_{R,1}\, sin\, \theta_{R,1} \quad \text{and} \quad \Delta_{y,2} = \Delta_{R,2}\, sin\, \theta_{R,2} \quad (9)$$

Where: $\Delta_{R,1}$ and $\Delta_{R,2}$ are the resultant displacements at shear studs 1 and 2 respectively; $F_{R,1}$ and $F_{R,2}$ are resultant forces at shear studs 1 and 2 respectively; $F_{x,1}$ and $F_{x,2}$ are the x-axis components of force at shear studs 1 and 2 respectively; $F_{y,1}$ and $F_{y,2}$ are the y-axis components of force at shear studs 1 and 2 respectively; $\theta_{R,1}$ and $\theta_{R,2}$ are the angles of the resultant forces on shears stud 1 and 2 respectively; k_s is stiffness of the shear studs.

Using the equations above and the averaged back-bone force-displacement response of the WSP connection in J01, as shown in Figure 6 (left), the nonlinear force-displacement behaviour of the individual shear studs was approximated and has been shown in Figure 6 (right).

The stiffness of the shear studs can be calculated using Equation 10 below, which is derived by substituting Equations 3–9 into Equation 2.

$$k_s = (1/\Delta_v)[F_{R,1}\, sin\, \theta_{R,1} + F_{R,2}\, sin\, \theta_{R,2} + (F_{R,1}\, cos\, \theta_{R,1} - F_{R,2}\, cos\, \theta_{R,2})(L/x)] \quad (10)$$

As discussed previously, the stiffness of the connection (i.e. k_v) was taken as the secant stiffness of the point corresponding to 70% of the maximum capacity being developed; which was 44.4 kN/mm for the WSP connections in J01. The individual stud stiffness at this point, using Equation 10, was then calculated to be approximately 170 kN/mm. This individual stud stiffness can then be used to extrapolate the connection stiffness for larger WSP connections with more than two shear studs.

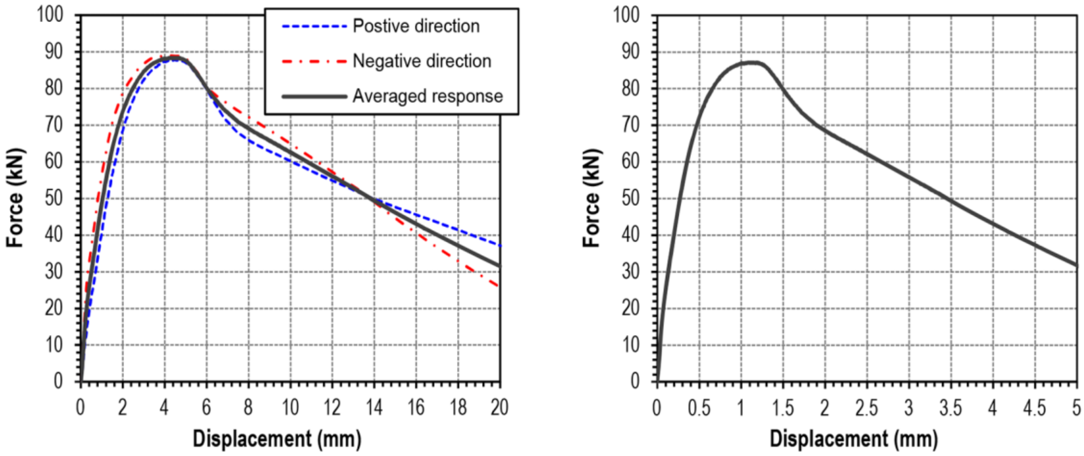

Figure 6: Backbone force-displacement response (left) and non-linear response of shear studs (right).

4 PROPOSED TYPICAL CONNECTIONS

A series of proposed WSP connections are presented in Figure 7, which include two, three, four and six shear stud options. The strength (i.e. ϕV_u) and stiffness (i.e. k_v) of each WSP configuration is presented in Table 1. The connection strengths given in Table 1 are based on the shear studs being the critical component of the connection and as such, are the forces required to develop the ultimate shear strength in the critical shear stud for each respective stud configuration, which was 79 kN (i.e. $\phi V_s = 0.85 \times 93 = 79$ kN), in accordance with AS 2327.1. The individual stud loading is calculated using Equations 11 and 12 below.

$$F_{x,i} = (Fey_i)/\sum_{i=1}^{n}\left(x_i^2 + y_i^2\right) \tag{11}$$

$$F_{y,i} = F/n + (Fex_i)/\sum_{i=1}^{n}\left(x_i^2 + y_i^2\right) \tag{12}$$

Where: F is the force acting on the connection; $F_{x,i}$ and $F_{y,i}$ are the x- and y-axis components of force on i-th stud respectively; n is the number of studs in the stud group; e is the eccentric of the stud group, which is equal to the distance from the centroid of the stud group to the point of contraflexure (i.e. zero moment), or more simply, the centre of a symmetric connection ($e = 0.5L$ in relation to Figure 5); x_i and y_i are the x- and y-axis distances to the i-th stud respectively.

The vertical connection stiffness was calculated using the stud stiffness of 170 kN/mm calculated in the previous section and assuming rigid body rotation of the connection, similar to the what was described in the previous section and shown in Figure 5. Further details can be found in Menegon (2018).

Table 1: Proposed WSP connection capacities.

Stud configuration	Shear capacity	Connection stiffness
2 x 1	89 kN	55 kN/mm
3 x 1	160 kN	144 kN/mm
2 x 2	152 kN	149 kN/mm
3 x 2	281 kN	329 kN/mm

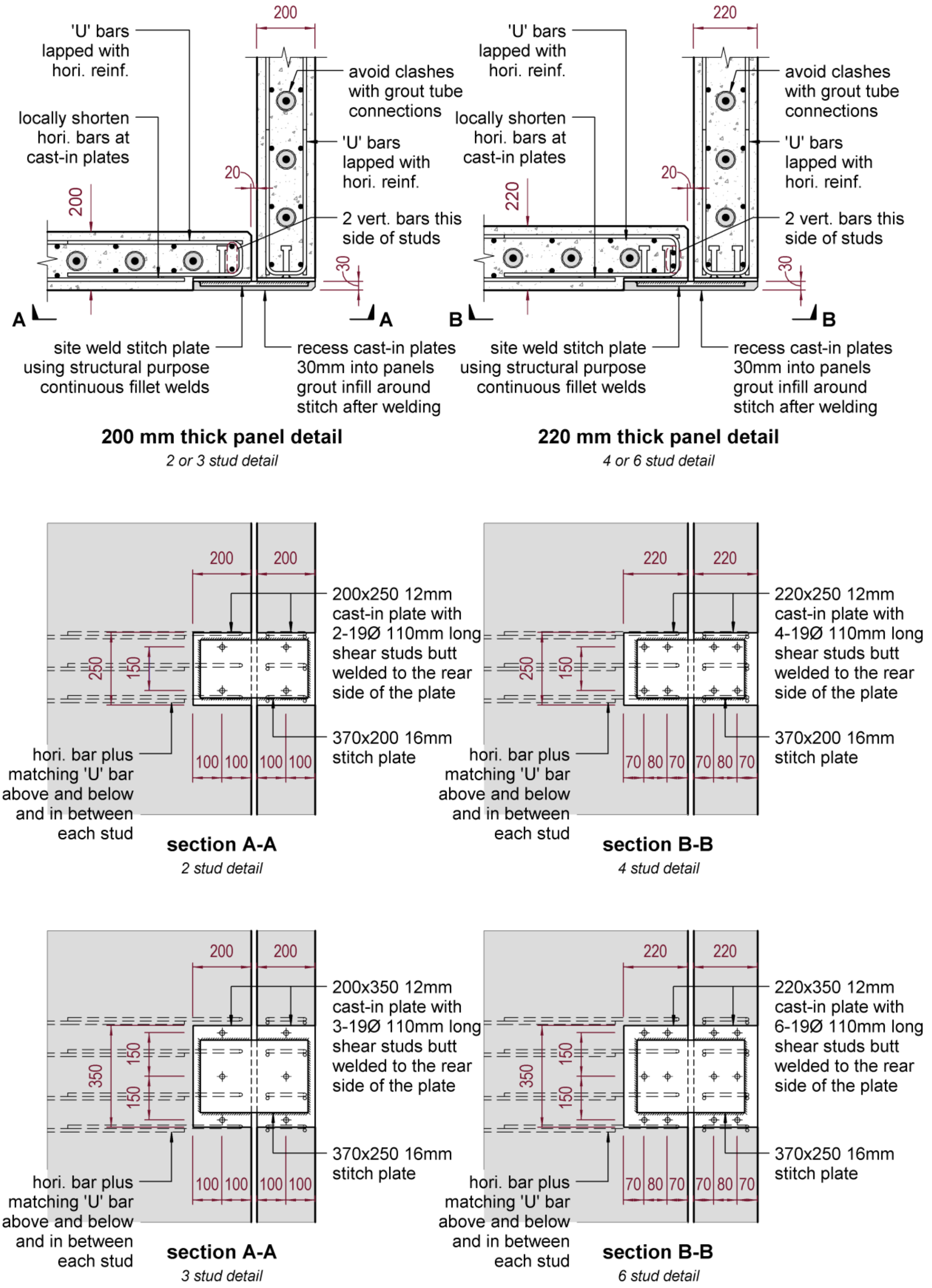

Figure 7: Proposed welded stitch plate connections.

5 SUMMARY AND CONCLUSIONS

This paper has presented a brief overview and the findings of a recent experimental study into welded stitch plate (WSP) connections in jointed precast building cores. The study included a full-scale test of a typical WSP connection, which is similar to what is specified/used in many Australian RC wall buildings. The connection was a 2-stud connection, which comprised of 19 mm diameter shear studs. The connection was able to develop a maximum capacity of 88 kN. The failure mechanism of the connection was yielding and subsequent fracturing of the shear studs. The connection underwent approximately 4 to 5 mm of movement prior to reaching its maximum strength and failing. The movement was dominated by rigid body rotation of the entire WSP connection. This allowed the non-linear force-displacement response curve of an individual single shear stud to be estimated. An approximated linear elastic stiffness of the 19 mm shear stud's movement in the concrete was estimated to be about 170 kN/mm. The paper is concluded with a series of proposed WSP connections for jointed precast building cores together with the associated maximum vertical shear capacities and connection stiffnesses.

6 ACKNOWLEDGEMENTS

Financial support from the Australian Research Council (ARC) Discovery Project DP180101593 entitled *Seismic Performance of Precast Concrete Buildings for Lower Seismic Regions* is gratefully acknowledged.

7 REFERENCES

Menegon, S.J. 2018. *Displacement Behaviour of Reinforced Concrete Walls in Regions of Lower Seismicity*, Doctor of Philosophy thesis, Department of Civil and Construction Engineering, Swinburne University of Technology.

Menegon, S.J., Wilson, J.L., Hughes, S. & Gad, E.F. 2017a. Experimental testing of precast connections for jointed precast building cores, *Proceedings of the Australian Earthquake Engineering Society 2017 Conference, November 24-26*, Canberra, ACT.

Menegon, S.J., Wilson, J.L., Hughes, S. & Gad, E.F. 2018a. The Development of Two New Innovative Precast Building Core Connections, *Proceedings of the Australasian Structural Engineering Conference, 25-28 September 2018*, Adelaide, Australia.

Menegon, S.J., Wilson, J.L., Lam, N.T.K. & Gad, E.F. 2017b. Comprehensive Experimental Testing Program of Limited Ductile Reinforced Concrete Walls, *Proceedings of the Australian Earthquake Engineering Society 2017 Conference, November 24-26*, Canberra, ACT.

Menegon, S.J., Wilson, J.L., Lam, N.T.K. & Gad, E.F. 2017c. RC Walls in Australia: Reconnaissance Survey of Industry and Literature Review of Experimental Testing, *Australian Journal of Structural Engineering*, Vol 18(1) 24-40.

Menegon, S.J., Wilson, J.L., Lam, N.T.K. & Mcbean, P. 2018b. RC Walls in Australia: Seismic Design and Detailing to AS 1170.4 and AS 3600, *Australian Journal of Structural Engineering*, Vol 19(1) 67-84.

Seifi, P., Henry, R.S. & Ingham, J.M. 2016. Panel Connection Details in Existing New Zealand Precast Concrete Buildings, *Bulletin of the New Zealand Society for Earthquake Engineering*, Vol 49(2) 190-199.

Standards Australia. 2003. *AS 2327.1-2003 Composite Structures, Part 1: Simply supported beams*, Standards Australia, Sydney, NSW.